ELSEVIER

Biochimica et Biophysica Acta 1509 (2000) 429–439

BIOCHIMICA ET BIOPHYSICA ACTA
BBA

www.elsevier.com/locate/bba

Functional characterization of purified zinc transporter from renal brush border membrane of rat

Rajinder Kumar, Rajendra Prasad *

Department of Biochemistry, Postgraduate Institute of Medical Education and Research, Chandigarh 160 012, India

Received 23 May 2000; received in revised form 29 August 2000; accepted 31 August 2000

Abstract

Major zinc binding protein purified from renal brush border membrane (BBM) (R. Kumar, R. Prasad, Biochim. Biophys. Acta 1419 (1999) 23) was reconstituted into liposomes and its functional characteristics were investigated. Physical incorporation of the major zinc binding protein into the proteoliposomes was checked by SDS–PAGE, which showed a single band on silver staining. The structural integrity of the proteoliposomes was assessed by phase contrast microscopy, which revealed the proteoliposomes as globular structures and intact boundaries. Further structural integrity/leakiness of the proteoliposomes was checked by monitoring efflux of Zn^{2+} from the pre-loaded proteoliposomes in the presence of either 2 mM Ca^{2+} or Cd^{2+} or Zn^{2+}. It was observed that even after 2 h of the initiation of efflux, 85–95% of Zn^{2+} was retained in the proteoliposomes, thereby indicating that proteoliposomes were not leaky and maintained structural integrity during the uptake study. Zinc uptake into the proteoliposomes followed Michaelis–Menten kinetics with affinity constant (K_m) of 1.03 mM and maximal velocity (V_{max}) of 1333 nmol/mg protein per min. The uptake process followed first-order kinetics with a rate constant (k) of 1.09×10^{-3} s^{-1}. The specificity of zinc transport system was determined by studying the interaction of divalent cations viz. Ca^{2+} and Cd^{2+} with the zinc uptake. It was observed that Cd^{2+} competitively inhibited the zinc uptake process with inhibitory concentration (K_i) of 2.9 mM. Kinetic analysis of inhibitory effect of Cd^{2+} on zinc uptake revealed an increase in K_m to 1.74 mM without influencing V_{max}. Zn^{2+} uptake into the proteoliposomes was found to be temperature sensitive and Arrhenius plot showed a breakpoint at 27°C. The apparent energies of activation (E_a) were found to be 7.09 and 2.74 kcal/mol below and above the breakpoint, respectively. The initial velocity of Zn^{2+} uptake increased with the increase in outwardly directed proton gradient ($[H]_i$ greater than $[H]_o$). The Zn^{2+} uptake was inhibited by DCCD, thereby suggesting the involvement of –COOH groups in the translocation of Zn^{2+} across the lipid bilayer. The ratio of acidic to basic amino acids (1.26) strongly indicates that it is an acidic protein. The cysteine content in this protein was insignificant, which further corroborates the possibility that the acidic amino acids might be prominent candidates for binding to zinc. The findings of the present study confirms that 40 kDa major zinc binding glycoprotein purified from renal BBM is a zinc transporter involved in the influx of Zn^{2+} into the epithelial cells of the renal tubular system.

Keywords: Major zinc binding protein; Kinetic constant; Proteoliposome; Zinc transporter; Zinc influx; Rat kidney cortex

1. Introduction

Metal ions are essential cofactors for a number of biological processes, including gene homeostasis.

* Corresponding author. Fax: +91-172-744401/745078; E-mail: fateh1977@yahoo.com

0005-2736/00/$ – see front matter
PII: S0005-2736(00)00325-4

Failure to maintain appropriate levels of metal ions in humans is feature of hereditary hemochromatosis [1], disorder of metal ions deficiency and certain neurodegenerative diseases [2]. Zinc-associated genetic disorders like acrodermatitis enteropathica, familial hypozincemia in humans and adema (trait A-46) in cattle have been thought possibly due to defects in zinc transport systems. Zinc is a small hydrophilic charged species, which cannot cross biological membranes by passive diffusion. Therefore, specialized mechanisms are required for both its uptake and release. Recent studies have established the importance of the renal brush border membrane (BBM) as a determinant of solute transport in proximal tubules [3–5]. Kinetic characteristics of zinc transport process have been described in many model systems including intact animals, isolated cells from various sources, intestinal segments, intestinal and renal BBM vesicles (BBMV) [4–8]. Recently four genes termed as zinc transporters (ZnT) have been cloned and characterized. These genes predict putative proteins with multiple membrane spanning domains and all have histidine rich intracellular loop. These transporters are organ specific and are involved in the specialized function of zinc transport. ZnT-1 and ZnT-4 are involved in the efflux of zinc in intestine, kidney tubules, mammary epithelium and synaptic vesicles [9,10]. ZnT-2 and ZnT-3 have been shown to be involved in the translocation of zinc from the cytosol to endosomal/lysosomal vesicles in the intestine, kidney, testis and brain [11,12]. The divalent cation transporter (DCT-1) is regulated by iron but exhibit transport activity for a number of other trace elements including zinc [13]. Interestingly, none of the transporters described so for has been reported to be involved in the uptake of zinc into the cells. A recent study in our laboratory on zinc uptake into the BBMV prepared from rat renal cortex has revealed the presence of extravesicular as well as intravesicular zinc binding sites [8]. A 40 kDa major zinc binding protein has been purified from renal BBM and physicochemically characterized [14]. Immunofluorescence staining localized the protein mainly in proximal tubules indicating its role in the zinc transport [14]. However, the functional characteristics of this protein were yet to be investigated. Here we present the functional characterization of the purified 40 kDa major zinc binding protein after reconstituting it into the liposomes. The findings of the present study suggested that the 40 kDa major zinc binding protein is a zinc transporter in the renal tubular system, involved in the influx of zinc into the cells.

2. Materials and methods

2.1. Chemicals

$^{65}ZnCl_2$ (specific activity, 536 mCi/g Zn^{2+}) was purchased from Bhabha Atomic Research Center, Trombay, Mumbai, India. *N′*-2-hydroxy-ethylpiperazine-*N*-2-ethanesulfonic acid (Hepes), Ethylene glycol bis(aminoethyl ether)-*N,N,N′N′*-tetraacetic acid (EDTA), egg yolk phosphatidyl choline (PC), and cholesterol were purchased from Sigma chemical Co. (St. Louis, MO, USA). Cellulose nitrate membranes (0.23 μm pore size) were obtained from Millipore Corporation (Bedford, MA, USA). All other chemicals were analytical reagent grade compounds from standard commercial sources.

2.2. Animals

Young male Wistar strain rats, weighing 150–200 g, were procured from the animal breeding colony of the institute. The animals were acclimatized to the laboratory conditions before commencement of the experiment. The animals were kept under hygienic conditions and fed standard rat pallet diet (Ashirbad, Chandigarh, India) and were given water ad libitum.

2.3. Purification of major zinc binding protein from renal BBM

The animals were killed under light ether anesthesia and renal BBM were prepared by differential centrifugation procedure as described earlier [3,4,8]. A 40 kDa major zinc binding glycoprotein was purified as described by us previously using different chromatography procedures and purity of the protein was checked by sodium dodecyl sulfate–polyacrylamide gel electrophoresis (SDS–PAGE) [14].

2.4. Preparation of proteoliposomes

Purified 40 kDa major zinc binding protein was

reconstituted into the liposomes by the method as described by Richard et al. [15] and Kumar and Prasad [16]. Five mg of purified protein was concentrated to one ml in Amicon ultrafiltration assembly using 10 kDa cut-off membrane and equilibrated with KHT buffer (150 mM KCl, 20 mM Hepes, 15 mM Tris, 0.2 mM EGTA, pH 6.9) to remove the excess of the *n*-octylglucoside (non-ionic detergent used in the purification protocol). Thirty-six mg of egg yolk PC and 9 mg cholesterol were dissolved in 1.0 ml of chloroform/methanol solution (2:1) under 100% N_2 atmosphere in a round-bottomed flask. The solvent was evaporated under reduced pressure with rota-vapor. The complete removal of the solvent was achieved by further evaporation under high vacuum with a N_2 trap. The thin film so obtained was suspended in 1.0 ml of KHT buffer with a small magnetic stirring bar. The milky suspension was transferred into a test tube. All the above steps were conducted under N_2 atmosphere. 1.0 ml of the sonicated lipids (pre-formed liposomes) was then frozen in liquid nitrogen and thawed at room temperature prior to the addition of the dialyzed protein. After addition of 1.0 ml of KHT buffer, the suspension was dialyzed at 4°C for 36–48 h against KHT buffer giving changes every 10–12 h. After dialysis, the suspension was diluted to 8.0 ml with reconstitution buffer (300 mM mannitol, 25 mM Hepes, pH 6.9) and centrifuged for 10 min at $1000 \times g$ to remove any aggregated material. The resulting supernatant was centrifuged for 1 h at $100\,000 \times g$ at 4°C to sediment the proteoliposomes. The pallet was resuspended in 1.0 ml of reconstitution buffer and gently homogenized by aspirating the suspension into a 1.0-ml syringe through a 26-gauge needle. This step was repeated three times. Similarly, liposomes were also subjected to the above procedure but without the addition of protein and finally reconstituted in 1.0 ml of the same buffer. Physical incorporation of the protein into the proteoliposomal membranes was checked by SDS–PAGE using Laemmli buffer system as described by us earlier [16].

2.5. Phase contrast microscopy

The proteoliposomes were viewed under the phase contrast microscope in order to assess the structural integrity. The proteoliposomes were diluted suitably, one drop was kept on the coverslip and it was inverted onto the glass slide. The microscope was kept on for 10 min before viewing the sample and the proteoliposomes were viewed under light and dark fields and photographed.

2.6. $^{65}Zn^{2+}$ efflux assay

The structural integrity/leakiness of the proteoliposomes was checked by chasing the efflux on $^{65}Zn^{2+}$ form the pre-loaded proteoliposomes. Proteoliposomes were pre-loaded with $^{65}Zn^{2+}$ by incubation for 2 h at 20°C in loading buffer (300 mM mannitol, 25 mM Hepes buffer (pH 6.9), 3.0 mM Zn^{2+} and 1.0 μCi $65Zn^{2+}$). One hundred μl of the pre-loaded proteoliposomal suspension (4–5 μg protein) was then diluted with 2.5 μl of buffer containing 300 mM mannitol, 25 mM Hepes, 2.0 mM Ca^{2+} or 2.0 mM Cd^{2+} or 2.0 mM Zn^{2+}. The reaction was stopped at various intervals by addition of 4.0 ml of ice-cold stop buffer (150 mM KCl, 25 mM Hepes, 5.0 mM EGTA (pH 6.9)). Then the filters were washed three times with the same buffer and the radioactivity retained on the filters was counted.

2.7. Transport measurements

2.7.1. Time course of zinc uptake

Uptake of zinc into the reconstituted liposomes was measured by the rapid filtration technique as described previously [4,8,16]. In brief, 20 μl of proteoliposomes (3–5 μg protein) was incubated at 20°C in 80 μl of uptake buffer (300 mM mannitol, 25 mM Hepes buffer (pH 6.9) containing 1.0 mM Zn^{2+} with 1.0 μCi of $^{65}Zn^{2+}$) for different time intervals and the reaction was stopped by the addition of 4.0 ml of ice-cold stop buffer consisting of 150 mM KCl, 25 mM Hepes buffer (pH 6.9) and 5.0 mM EGTA. The filters were then rinsed three times with same stop solution. Radioactivity retained of the filters was measured by an Autogamma scintillation counter (1282 Compugamma, Universal Gamma Counter).

2.7.2. Kinetic constants measurements

In order to determine the kinetic constants (i.e., K_m and V_{max}, initial velocity) uptake of zinc was measured in the proteoliposomes. Twenty microliter of proteoliposomes (3–5 μg protein) were incubated

at 20°C with 80 μl of uptake buffers containing increasing concentrations of Zn^{2+} (0.5–3.0 mM) and 1.0 μCi of $^{65}Zn^{2+}$. After 30 s of incubation, the uptake was stopped by 40-fold dilution with ice-cold stop buffer. The vesicles were filtered and rinsed with the same buffer and the radioactivity retained on the filters was measured. Uptake of Zn^{2+} was also measured in the presence of 2.0 mM Ca^{2+} or Cd^{2+} in the incubation medium to check the specificity of the transporter for the zinc.

2.7.3. Effect of pH on the Zinc uptake

Zinc uptake into the proteoliposomes was measured as a function of pH at initial velocity conditions. Uptake of Zn^{2+} was measured at 20°C in the presence of different pH gradients as described in Section 2.7.1. After reconstituting the proteoliposomes in the reconstitution buffers with increasing pH (2.9, 3.9, 4.9, 5.9 or 6.9), the uptake of Zn^{2+} was measured in 100 μl of uptake buffer (pH 6.9) so that $[H^+]_i > [H^+]_o$. Similarly, the uptake of Zn^{2+} into the proteoliposomes reconstituted in the buffer with pH 6.9 was measured in the uptake buffer of increasing pH (2.9, 3.9, 4.9, 5.9 or 6.9) so that $[H^+]_i < [H^+]_o$.

2.7.4. Influence of temperature on zinc uptake

Initial velocity of zinc uptake was measured at different temperatures (10–45°C) in the presence of 1.0 mM Zn^{2+} and 1.0 μCi of $^{65}Zn^{2+}$ in the incubation buffer as described in Section 2.7.1. An Arrhenius plot was constructed on the basis of the results so obtained. From the slope of lines, the activation energies (E_a) were calculated using the Arrhenius equation.

2.7.5. Effect of –SH and –COOH blockers on zinc uptake

To assess the involvement of sulfhydryl and carboxyl groups in the transport of zinc across the lipid bilayer, the initial velocity of zinc uptake was measured in the presence of 5.0 mM of DCCD (–COOH groups blocker) or iodoacetate (–SH groups blocker) as described in Section 2.7.1.

2.8. Amino acid composition

The amino acid composition of the purified protein was analyzed by the method of DuVal and Fowler [17]. Purified major zinc binding protein was hydrolyzed in Vacuo at 110°C for 24 h with twice-distilled HCl. Half cysteine was determined as cystic acid after performic acid oxidation. Hydrolysate samples were neutralized with triethylamine and derivatized with phenylisothiocyanate. Amino acid analysis was done on Water's PICO tag amino acid analyzer calibrated with amino acids standard.

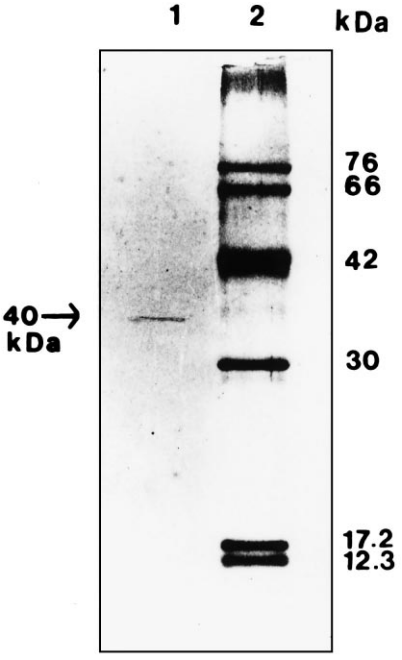

Fig. 1. SDS–PAGE of proteoliposomes reconstituted with purified major zinc-binding protein. The protein samples were resolved on 12% acrylamide gel. Lane 1, proteoliposomes reconstituted with major zinc-binding protein (0.5 μg); lane 2, standard molecular mass markers. Protein bands were visualized by silver nitrate staining.

2.9. Statistical analysis

All values presented in this study are the mean ± S.D. of at least six measurements on three or more separate proteoliposomal preparations.

3. Results

3.1. SDS–PAGE

Reconstituted proteoliposomes were analyzed on

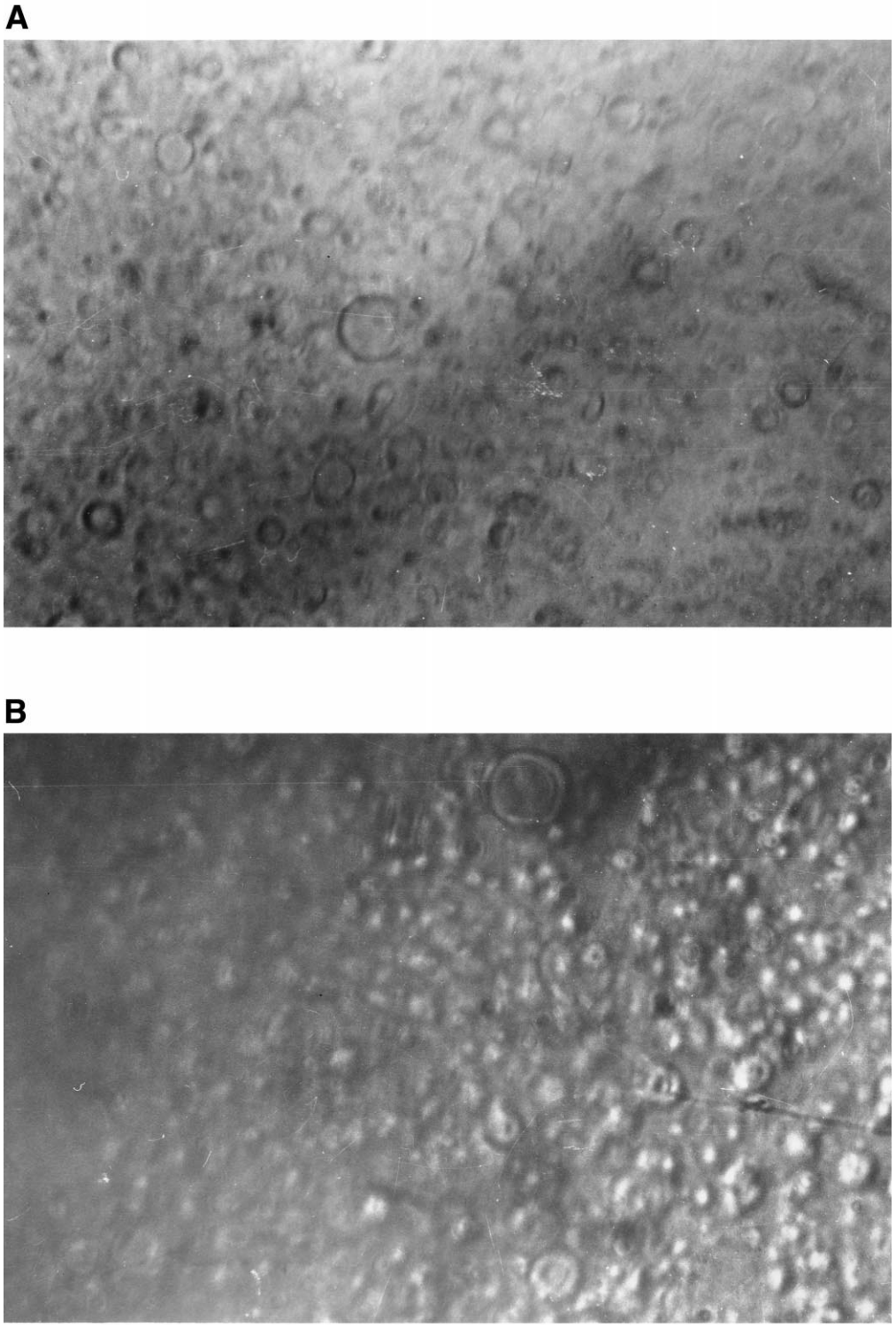

Fig. 2. Photomicrograph of proteoliposomes. Vesicularity of the proteoliposomes was checked by phase contrast microscopy. The Proteoliposomes were viewed under light field (A: ×400) and dark field (B: ×400).

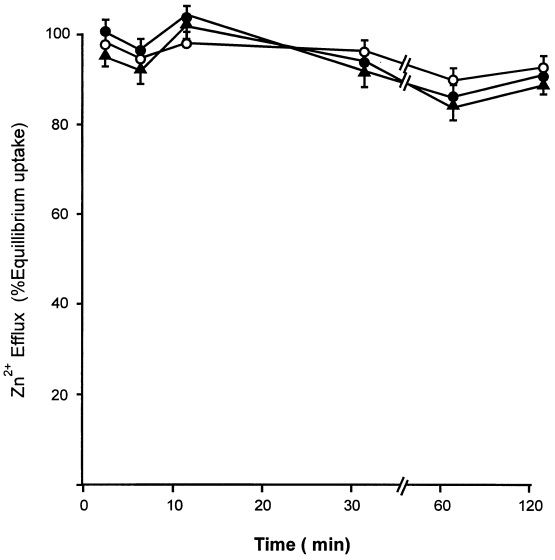

Fig. 3. Efflux of zinc from the proteoliposomes reconstituted with purified major zinc binding protein. Proteoliposomes were pre-loaded with $^{65}Zn^{2+}$ by incubation for 2 h at 20°C in loading buffer (300 mM mannitol, 25 mM Hepes buffer (pH 6.9), 3.0 mM Zn^{2+}, 1.0 μCi $^{65}Zn^{2+}$). One hundred μl of pre-loaded proteoliposomal suspension (4–5 μg protein) was then diluted with 2.5 ml of buffer containing 300 mM mannitol, 25 mM Hepes, 2 mM Ca^{2+} (●), 2 mM Cd^{2+} (○) or 2 mM Zn^{2+} (▲). The reaction was stopped at various intervals by addition of 4.0 ml of ice-cold stop buffer (150 mM KCl, 25 mM Hepes, 5 mM EGTA (pH 6.9)). Then the filters were washed three times with the same buffer. The values are mean ± S.D. of five independent experiments, each carried out in triplicate.

SDS–PAGE using 12% gel (Fig. 1). The reconstituted proteoliposomal protein showed a single band with electrophoretic mobility of 40 kDa, thereby indicating that the major zinc binding protein has been reconstituted into the proteoliposomes.

3.2. Phase contrast microscopy

Structural integrity of proteoliposomes was checked by phase contrast microscopy (Fig. 2). It can be seen that all the proteoliposomes are unilamellar and their boundaries are intact. The proteoliposomes were more or less of the same shape and size. Under the dark field the proteoliposomes appeared as globular structures (Fig. 2B).

3.3. Zinc efflux study

To check further the structural integrity/leakiness of the proteoliposomes, efflux of zinc from preloaded proteoliposomes was monitored in the presence of different divalent cations, viz., 2.0 mM Ca^{2+}, Cd^{2+} or Zn^{2+} (Fig. 3). It is clearly shown that even after 2 h of the initiation of the efflux, 85–90% of the zinc was retained in the proteoliposomes in the presence of either of the cations. These findings confirmed the intactness of the proteoliposomes during the uptake study.

3.4. Kinetic characterization of zinc uptake into the proteoliposomes

Zinc uptake increased progressively with time and reached equilibrium at 2 h of incubation (Fig. 4). Therefore, initial velocity zinc uptake was measured at 30 s in the further studies.

To determine the kinetic constants of zinc uptake process, zinc uptake into the proteoliposomes was measured in the presence of increasing substrate concentrations. The zinc uptake as a function of substrate concentration followed Michaelis–Menten kinetics, showing a typical hyperbola, reaching satu-

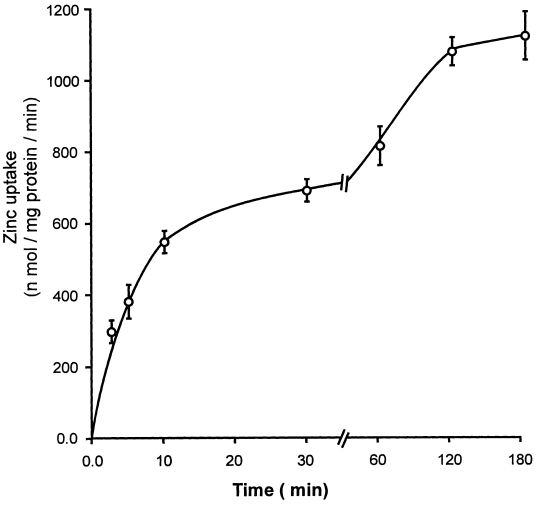

Fig. 4. Time course of zinc uptake into the proteoliposomes reconstituted with purified major zinc binding protein. Uptake of zinc was measured at 1 mM extravesicular Zn^{2+} in uptake buffer (300 mM mannitol, 25 mM Hepes buffer (pH 6.9), 1.0 μCi $^{65}Zn^{2+}$) for different time intervals. The reaction was stopped by addition of 4.0 ml of ice-cold stop buffer (150 mM KCl, 25 mM Hepes, 5 mM EGTA (pH 6.9)). The filters were washed three times with the same buffer and radioactivity retained on the filters was counted. The values are mean ± S.D. of five or more independent experiments, each carried out in triplicate.

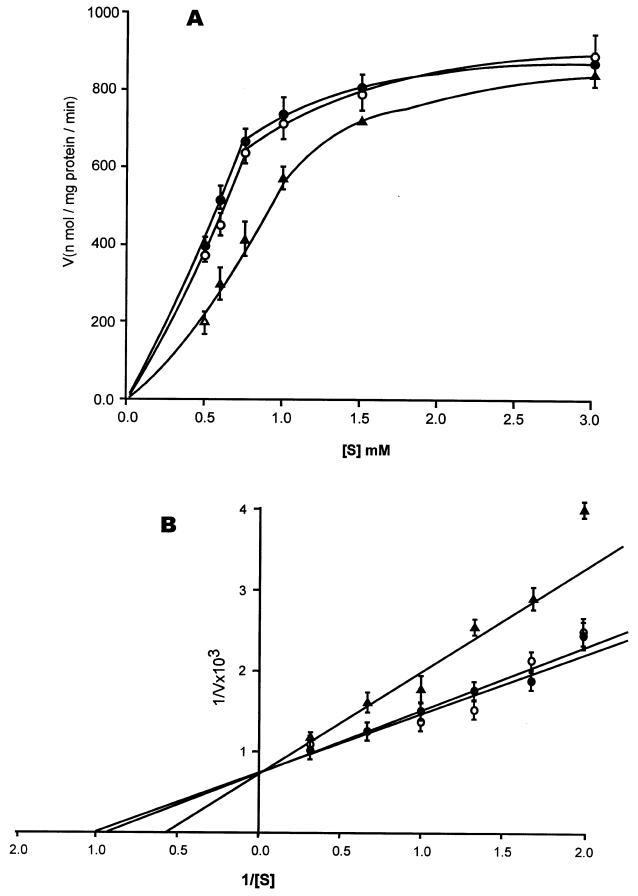

Fig. 5. Substrate dependence of zinc uptake into the proteoliposomes reconstituted with major zinc binding protein. (A) Initial velocity of zinc uptake was measured in the presence of different extravesicular zinc concentrations (0.5–3.0 mM) in the uptake buffer (300 mM mannitol, 25 mM Hepes buffer (pH 6.9), 1.0 μCi $^{65}Zn^{2+}$] in the absence (▲) or presence of 2 mM Cd^{2+} (○) or 2 mM Ca^{2+} (●). (B) Lineweaver–Burk plot, which is transformed from A; K_m and V_{max} were determined by linear regression analysis of data. K_i and k were calculated from these data. The results are expressed as mean ± S.D. of four experiments, each carried out in triplicate with different proteoliposomal preparations.

ration at 2.5 mM of zinc (Fig. 5A). These data were then transformed into a Lineweaver–Burk plot (Fig. 5B), which revealed K_m of 1.03 mM and V_{max} of 1333 nmol/mg protein per min. Zinc uptake followed first-order kinetics and k was found to be 1.09×10^{-3} s^{-1} (Table 1).

3.5. Interaction of divalent cations viz. Ca^{2+} and Cd^{2+} with zinc uptake

To study the interaction of divalent cations with zinc transport, the zinc uptake into the proteoliposomes was measured in the presence of either 2.0 mM Ca^{2+} or Cd^{2+} (Fig. 5B). Zinc uptake was found to be inhibited by Cd^{2+}, whereas Ca^{2+} did not show any effect on zinc uptake. Cd^{2+} resulted in a significant decrease in affinity of the transporter for zinc, although no effect was observed on maximal velocity of zinc uptake. Kinetic inhibitory concentration of Cd^{2+} was found to be 2.9 mM and first-order constant was observed to be decreased significantly (Table 1).

3.6. Effect of pH on zinc uptake

The effect of proton gradient of the zinc uptake is shown in Fig. 6. The proteoliposomes were reconstituted in the buffers of varying pH and Zn^{2+} uptake into the proteoliposomes was measured in the uptake buffer of pH 6.9 ($[H^+]_i$ greater than $[H^+]_o$). A marked stimulation in the initial velocity of zinc uptake was observed with increasing proton gradient, whereas a marked inhibition in the rate of zinc uptake was observed when the proteoliposomes equilibrated in a buffer of pH 6.9 were incubated in the reaction mixture of increasing pH so that $[H^+]_i$ less than $[H^+]_o$.

Table 1
Kinetic constants of zinc uptake into the proteoliposomes reconstituted with purified major zinc-binding protein

Sample no.	Metal	K_m (mM)	V_{max} (nmol/mg protein per min)	K_i (mM)	k (s^{-1})
1	$Zn2^+$	1.03	1333	–	1.09×10^{-3}
2	Ca^{2+}	1.08	1325	–	1.02×10^{-3}
3	Cd^{2+}	1.74	1333	2.90	0.64×10^{-3}

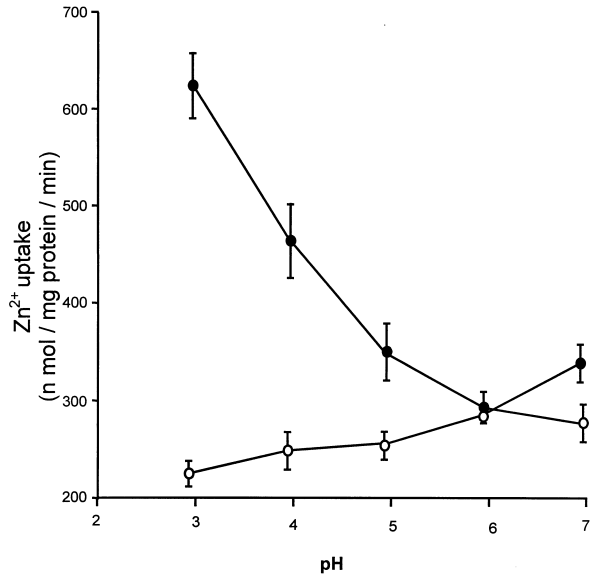

Fig. 6. Effect of pH on initial velocity of zinc uptake into the proteoliposomes reconstituted with purified major zinc binding protein. Effect of extravesicular pH (○): 20 μl (4–5 μg protein) of proteoliposomes reconstituted in a buffer containing 300 mM mannitol and 25 mM Hepes (pH 6.9) were incubated with 80 μl of uptake buffer (300 mannitol, 25 mM Hepes (pH 2.9, 3.9, 4.9, 5.9 or 6.9), 1.0 mM Zn^{2+} and 1.0 μCi $^{65}Zn^{2+}$). Effect of intravesicular pH (●): 20 μl of proteoliposomes (4–5 μg protein) reconstituted in buffers of different pH (2.9, 3.9, 4.9, 5.9 or 6.9) were incubated with 80 μl of uptake buffer (pH 6.9) at 20°C. At 30 s, the reaction was terminated by addition of 4.0 ml of ice-cold stop buffer. Data are presented as mean ± S.D. of five independent experiments, each carried out in triplicate.

3.7. Influence of temperature on zinc uptake

An increase in zinc uptake was observed with the increase in incubation temperature from 10°C to 45°C as depicted in Fig. 7. Arrhenius plot showed a breakpoint at 27°C and the energies of activation (E_a) were found to be 7.09 kcal/mol and 2.74 kcal/mol below and above the break point, respectively.

3.8. Effect of –SH and –COOH blockers on the zinc uptake

In the presence of –SH group blocker, viz., iodoacetate, initial velocity of zinc uptake was observed to be inhibited by 8% as compared to control. However, 40% inhibition in zinc uptake was seen in the presence of DCCD, a –COOH groups blocker. Further, proteoliposomes were pre-incubated with antisera raised against the purified zinc binding protein and zinc uptake was measured at initial velocity conditions. It was found that Antibodies at a dilution of 1:10 resulted in 53% inhibition, whereas 47% inhibition was noticed at the dilution of 1:50.

3.9. Amino acids composition of purified zinc binding protein

The purified protein was analyzed for the amino acid composition in Waters PICO tag amino acid analyzer. Free amino acid standards were used for the identification of amino acid composition of the protein (Table 2). It was found that out of 380 amino acid residues, 129 residues were charged, i.e., arginine and lysine (57 residues) and aspartate and glutamate (72 residues). Protein is acidic in nature as indicated by the ratio of acidic to basic residues, which was found to be greater than 1. However, the protein has no cysteine residues. Interestingly, there is a high content of proline in the protein.

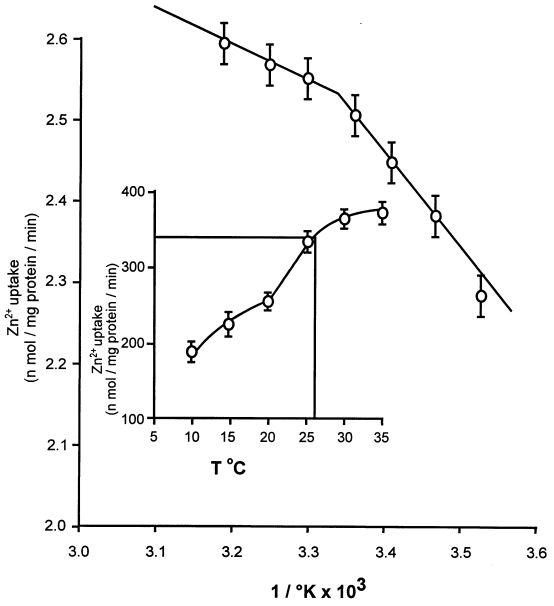

Fig. 7. Effect of temperature on zinc uptake into the proteoliposomes reconstituted with purified major zinc binding protein. Twenty μl (4–5 μg protein) of proteoliposomes were incubated with 80 μl of uptake buffer containing 1.0 mM Zn^{2+} and 1.0 μCi $^{65}Zn^{2+}$ at various temperatures (10–45°C). The data were plotted according to Arrhenius plot. All values are mean ± S.D. of the results obtained from 12 independent measurements from four different proteoliposomal preparations. E_a values were calculated by using the Arrhenius equation.

Table 2
Amino acid composition of purified major zinc binding protein

Amino acid	pmol	Residue	Int.
Aspartic acid	291.21	19.94	20
Serine	326.06	21.64	22
Histidine	41.68	2.74	3
Threonine	127.0	8.39	8
Proline	1078.48	71.25	71
Valine	242.91	16.05	16
1/2 Cystine	0.00	0.00	0
Leucine	370.06	24.45	24
Lysine	738.27	48.77	49
Hydroxy prol.	0.00	0.00	0
Glutamate	787.27	51.88	52
Glycine	629.99	54.64	55
Arginine	221.07	14.61	15
Alanine	310.59	20.52	21
Tyrosine	9.95	0.66	1
Methionine	42.87	2.89	3
Isoleucine	77.36	5.11	5
Phenylalanine	268.77	17.10	17
Tryptophan	0. 00	0.00	0
GABA	0.00	0.00	0
Unknown	0.00	0.00	0

pmol of peptide in original sample: 15.09; estimated length of peptide: 380; actual length of peptide: 381; average molecular mass range: 40 kDa.

4. Discussion

A family of related zinc transport proteins has been identified in mammals. The ZnT proteins are predicted to have similar structure, consisting of six transmembrane domains and a histidine-rich cytoplasmic loop. However, none of the transporters described so far has been shown to be involved in the influx of zinc into the cells. Recently we identified a 40 kDa major zinc binding protein from renal BBM which is the first barrier in the transepithelial movement of zinc [14]. Further studies were carried out to investigate the functional characteristics of this protein after reconstituting it into the proteoliposomes.

Physical incorporation of the purified major zinc binding protein into the proteoliposomes was evident from SDS–PAGE (Fig. 1) as has been reported for renal phosphate and Na^+/D-glucose cotransporter [18,19]. Structural integrity of the proteoliposomes was checked by phase contrast microscopy (Fig. 2) and Zn^{2+} efflux assay (Fig. 3). Phase contrast microscopy showed that the liposomes were unilamellar and boundaries were intact. Further, Zn^{2+} efflux assay showed that approximately 85–90% of Zn^{2+} was retained in the preloaded proteoliposomes even after 2 h of the initiation of efflux, thereby indicating that the proteoliposomes remained structurally intact during the uptake study. Structural integrity and unilamellar nature of the proteoliposomes are the prerequisite for the use of proteoliposomes in the transport measurements.

Kinetic characterization of zinc uptake into proteoliposomes showed a slight increase in the K_m of the transporter for zinc when compared with that reported for BBMV by Prasad et al. [8] (Table 1). The observed increase in K_m could be due to the change in the microenvironment of the protein in the proteoliposomes. However, there was an approximately 40-fold increase in V_{max}, which can be attributed to the presence of increased number of active transporter protein in the proteoliposomes. Further, the first-order rate constant was also found to be increased, thereby suggesting the increased rate of transport of zinc across the lipid bilayer in the proteoliposomes. These observations are in accordance with the earlier studies on reconstitution of purified renal phosphate transporter and Ca^{2+}-ATPase system into the proteoliposomes [18,20,21]. Carrier-mediated transport of solute is competitively inhibited by its structural analogues. Cadmium and zinc share some physicochemical properties and cadmium is a known competitive inhibitor of zinc transport process in the renal BBMV, renal proximal cells [3,8,22–24] and intestine [6,25]. Interaction of divalent cations, viz., Ca^{2+} and Cd^{2+}, with zinc uptake into the proteoliposomes was investigated. As expected, zinc uptake into the proteoliposomes was competitively inhibited by 2 mM Cd^{2+}, whereas Ca^{2+} did not show any effect on the zinc uptake. Ca^{2+} and Cd^{2+} did not behave in an analogous fashion at any point in the study, although both are divalent cations and they conceivably could share similar transport mechanisms. Our findings taken together indicate that zinc follows a very specific pathway to enter vesicles. This has also been reported earlier by Tacnet and co-workers [26], in that the Ca^{2+} ionophore A23187 (10 μM) had only a slight stimulating effect on the initial velocity of zinc uptake.

Temperature is one of the parameters that influen-

ces membrane-associated processes, such as membrane transport, enzymatic activities and membrane fusion [27–29]. The influence of the physical state of the membrane on the rate limiting step of the transport process can be deduced from the appearance of the break point in the Arrhenius plot and their correlation with thermotropic transitions of the transport systems [28]. The dependence of Zn^{2+} transport, Na^+,K^+-ATPase and D-glucose transport systems on temperature has been studied in intact BBMV and reconstituted vesicles [3,4,8,27,30]. In our study, temperature dependence of zinc transport into the reconstituted proteoliposomes showed a breakpoint at 27°C (Fig. 7). E_a has been found to be fivefold higher below the transition point than above. The high E_a below the phase transition is indicative of the fact that the transport system requires the lipids surrounding the protein to be in a mobile state in order to express its full activity [27]. E_a values determined for the reconstituted zinc transport system are comparable to those observed in rat renal BBMV above and below the break point as reported earlier [4,8]. These findings indicated that extraction of the transport protein from natural membrane and its subsequent reconstitution into lipid vesicles did not markedly change the characteristics or the energy requirements of the transport protein. These observations also indicate that the transport process is not very much influenced by the composition of the lipids surrounding the transport protein provided that appropriate membrane fluidity is achieved.

Zinc transport has been reported to be influenced by the proton gradient across the renal BBMV [4]. Therefore, Zn^{2+} uptake into the proteoliposomes reconstituted with purified major zinc-binding protein was measured in the presence of different proton gradients (Fig. 6). The increase in outwardly directed proton gradient enhanced the zinc uptake in contrast to inwardly directed proton gradient, which resulted in the decrease in zinc uptake. These results further substantiate the earlier observation that zinc uptake is influenced by an outwardly directed proton gradient in BBMV [4]. Recently, Gunshin and co-workers [13] have cloned and characterized a mammalian proton coupled metal-ion transporter (DCT-1), which has been shown to have a key role in the intestinal absorption of different metal ions including Zn^{2+}. DCT-1 mediates active transport that is proton coupled (symport) and depends on the cell membrane potential. However, our findings suggest the involvement of a Zn^{2+}/H^+ exchanger in the exchange of H^+ for Zn^{2+} across the BBM. The physiological significance of coupling of Zn^{2+} transport with H^+ could be attributed to the fact that coupling to the movement of H^+ down its electrochemical gradient will always ensure a concentrative uptake of Zn^{2+} even at trace amounts. Sulfhydryl groups have been shown to be involved in the Ca^{2+} transport and Na^+-phosphate co-transport in the intestinal and renal BBMV [31–33]. However, in our study Zn^{2+} uptake into the proteoliposomes was not affected by the presence of exofacial –SH groups blocking agents such as iodoacetate. Moreover, amino acid composition of purified protein did not reveal the presence of cysteine residues (Table 2). These findings suggest that –SH groups are not involved in Zn^{2+} transport. However, –SH-containing compounds such as β-mercaptoethanol resulted in a significant inhibition in Zn^{2+} uptake, demonstrating the prevention of sequestration of zinc to zinc carrier protein. These observations are in accordance with the earlier findings that small ligands such as cysteine and histidine inhibited the zinc uptake into renal proximal tubules in dog [34,35]. Interestingly, Zn^{2+} uptake into the proteoliposomes was found to be inhibited by –COOH groups modifying agents such as DCCD. These findings are further substantiated by the presence of high contents of –COOH groups containing amino acid residues, viz., glutamate and aspartate, in the purified major zinc binding protein, which are the possible candidates of Zn^{2+} binding in the absence of cysteine residues. These findings taken together demonstrated that Zn^{2+} transport could involve –COOH groups present in the protein on the exofacial surface. Zn^{2+} uptake at the initial velocity conditions was found to be inhibited by the antibodies raised against the purified protein, thereby suggesting that antibodies are binding to a specific domain of the protein which is directly or indirectly involved in the uptake of Zn^{2+} into the proteoliposomes. The findings of the present study suggest that the purified 40 kDa major zinc binding protein is a zinc transporter in the renal tubules, involved in the influx of zinc into the epithelial cells. Further studies are in progress to identify, clone and characterize the gene encoding this 40 kDa zinc transporter in order to further understand the

mechanism of zinc transport across the biological membranes.

Acknowledgements

We are thankful to Dr Vivek Kumar for valuable suggestions in preparation of the manuscript. This project was financed by the council of Scientific and Industrial Research, New Delhi, India (Sanction Number 37 (0957)/97/EMR-II).

References

[1] J. Feder, Nat. Genet. 13 (1996) 339–408.
[2] E.C. Hirsch, Mol. Neurol. 94 (1997) 135–142.
[3] R. Prasad, R. Nath, J. Trace Elem. Exp. Med. 6 (1993) 95–107.
[4] R. Prasad, V. Kumar, R. Kumar, K.P. Singh, Am. J. Physiol. 276 (1999) E774–782.
[5] J.G. Reyes, Am. J. Physiol. 270 (1996) C401–C410.
[6] M.P. Menard, R.J. Cousins, J. Nutr. 113 (1983) 1434–1442.
[7] F. Tacnet, D.W. Watkins, P. Ripoche, Biochim. Biophys. Acta 1024 (1990) 323–330.
[8] R. Prasad, D. Kaur, V. Kumar, Biochim. Biophys. Acta 1284 (1996) 69–78.
[9] R.D. Palmiter, S.D. Findley, EMBO J. 14 (1995) 639–649.
[10] L. Huang, J. Gitschier, Nat. Genet. 17 (1997) 292–297.
[11] R.D. Palmiter, T.B. Cole, S.D. Findley, EMBO J. 15 (1996) 1784–1791.
[12] R.D. Palmiter, T.B. Cole, C.J. Quaife, S.D. Findely, Proc. Natl. Acad. Sci. USA 93 (1996) 14934–14939.
[13] H. Gunshen, B. Mackenzie, U.V. Berger, Y. Guhnshin, M.F. Romero, W.F. Boron, S. Nussberges, J.L. Gollan, M.A. Hediger, Nature 388 (1997) 482–488.
[14] R. Kumar, R. Prasad, Biochim. Biophys. Acta 1419 (1999) 23–32.
[15] D. Richard, L. Klausner, J.V. Renswoude, Methods Enzymol. 104 (C) (1984) 340–347.
[16] R. Kumar, R. Prasad, J. Biochem. Mol. Biol. Biophys. 3 (1999) 27–37.
[17] G. DuVal, B.A. Fowler, Biochem. Biophys. Res. Commun. 159 (1989) 177–184.
[18] C. Schali, D.D. Fanestil, Biochim. Biophys. Acta 819 (1985) 66–74.
[19] P. Malathi, H. Preiser, Biochim. Biophys. Acta 735 (1983) 314–324.
[20] C. Schali, D.A. Vanghen, D.D. Fanestil, Biochem. J. 235 (1986) 189–197.
[21] V. Niggli, E.S. Adunyah, J.T. Penniston, E. Carafoli, J. Biol. Chem. 256 (1981) 395–401.
[22] E.C. Foulke, S. Blank, Toxicol. Appl. Pharmacol. 102 (1990) 464–473.
[23] B. Gachot, M. Tauc, L. Morat, P. Poujeol, Eur. J. Physiol. 49 (1991) 583–587.
[24] B. Gachot, M. Tauc, F. Wanston, L. Morat, P. Poujeol, Biochim. Biophys. Acta 1191 (1994) 292–298.
[25] G.W. Powel, W.J. Miller, J.D. Morton, C.M. Clifton, J. Nutr. 84 (1984) 205–215.
[26] F. Tacnet, F. Lauthier, P. Ripoche, J. Physiol. 465 (1993) 57–72.
[27] M.E.M. DaCruz, R. Kinne, J.T. Lin, Biochim. Biophys. Acta 732 (1983) 691–698.
[28] H. Sandermann Jr., Biochim. Biophys. Acta 515 (1978) 209–237.
[29] E.J. McMurchie, J.K. Raison, Biochim. Biophys. Acta 554 (1979) 364–374.
[30] R. Tanaka, A. Teruya, Biochim. Biophys. Acta 323 (1973) 584–591.
[31] R.B. Beechey, A.M. Roberton, C.T. Holloway, I.G. Knight, Biochemistry 6 (1967) 3867–3879.
[32] M. Loghman, Am. J. Physiol. 260 (1991) F874–F882.
[33] M. Loghman-Adam, G.T. Motock, P. Wilson, M. Levi, Am. J. Physiol. 269 (1995) F93–F102.
[34] D.K. Abuhamdam, S.D. Migdal, R. Whitehouse, P. Rubbani, A.S. Prasad, F.D. McDonald, Am. J. Physiol. 241 (1981) F487–F494.
[35] W. Victery, J.M. Swith, A.J. Vander, Am. J. Physiol. 241 (1981) F532–F539.